

N95-21754

33

395750

PUSHING THE LIMITS OF SPATIAL RESOLUTION WITH THE KUIPER AIRBORNE OBSERVATORY

D. LESTER

Department of Astronomy, University of Texas, Austin, TX 78712

THE PROBLEM OF HIGH SPATIAL RESOLUTION IN THE FAR- INFRARED

The study of astronomical objects at high spatial resolution in the far-IR is one of the most serious limitations to our work at these wavelengths, which carry information about the luminosity of dusty and obscured sources. At IR wavelengths shorter than $30\text{ }\mu\text{m}$, ground based telescopes with large apertures at superb sites achieve diffraction-limited performance close to the seeing limit in the optical. At millimeter wavelengths, ground based interferometers achieve resolution that is close to this. The inaccessibility of the far-IR from the ground makes it difficult, however, to achieve complementary resolution in the far-IR.

The 1983 IRAS survey, while extraordinarily sensitive, provides us with a sky map at a spatial resolution that is limited by detector size on a spatial scale that is far larger than that available in other wavelengths on the ground. The survey resolution is of order $4'$ in the $100\text{ }\mu\text{m}$ bandpass, and $2'$ at $60\text{ }\mu\text{m}$ (*IRAS Explanatory Supplement*, 1988). Information on a scale of $1'$ is available on some sources from the CPC. Deconvolution and image restoration using this database is one of the subjects of this workshop.

The highest spatial resolution in the far-IR has, however, for the last twenty years, been provided by the Kuiper Airborne Observatory (KAO). This telescope, in the fuselage of a C-141 transport plane based at NASA Ames Research Center, has been a mainstay for high resolution studies even preceding IRAS (Lester 1991). With optical components of quality high enough even for visible light studies, and commensurate tracking accuracy, diffraction-limited studies at far-IR wavelengths are possible ($\lambda/D=21''$ at $100\text{ }\mu\text{m}$). From the time of its commissioning in 1974 through the publication of the IRAS survey, most of the far-IR studies with this telescope were done on spatial scales of an arcminute or so, not even approaching that ultimately achievable. Nevertheless, it is worth pointing out that all far-IR photometry ever done on the KAO has been done on scales considerably smaller than that of the IRAS survey. While the diffraction-limited resolution of the KAO is more than a factor of ten higher than that provided by the IRAS survey, the switched-beam background cancellation with that telescope puts an upper limit on the spatial scale that is transmitted. The secondary chopper on the KAO can exceed amplitudes of $10'$, making for a spatial dynamic range of about 30 at $100\text{ }\mu\text{m}$.

The accessibility of the KAO to instrument development teams has made it an observatory with a continually evolving instrument complement. Here new instruments can progress from the drawing board to the stratosphere in less than a year, and the design of these instruments and the modifications to them, can

closely parallel, and directly address, timely astronomical questions. By virtue of its accessibility, the observatory promotes instrument development that is at the cutting edge of technology, where reliability and survivability is not a critical, expensive, and time-consuming proposition. High-risk, high payoff experiments are routinely accommodated. If an instrument doesn't work on one flight, it can more often than not be fixed before the next. It is reasonable to characterize the space IR astronomy that is done from the KAO in terms of the number of "launches" that it provides per year (about seventy).

CAPITALIZING ON THE SPATIAL RESOLUTION OF THE KAO IN THE FAR INFRARED

Starting in 1985, Paul Harvey and his team from the University of Texas made the first attempts to push the far-IR spatial resolution of the KAO to its ultimate limits. This required development of instrumentation with diffraction-limited detectors, and techniques for careful pointing. The first instrument to be used in this way was a three channel (0.8K bolometer) photometer, configured with diffraction-limited slits instead of large apertures. While the orientation of these slits on the sky was elevation and azimuth, careful flight planning allowed the slits to be scanned across astronomical sources at optimal angles.

It is important to understand that, while two dimensional spatial resolution is important, many of the most important questions in far-IR photometry hinge not so much on the detailed profile of an astronomical source, but simply on whether a large fraction of the luminosity of the source is from a component that is resolved at all. This question can easily be addressed with slit scans. For example, the optical depth (and hence dust column density) in a cloud, can be derived by comparison of its color temperature and brightness temperature. The latter requires an estimated size. The source of far-IR luminosity in galaxies with active nuclei remains a crucial problem and, for the more nearby galaxies, this problem can be reduced to whether the far-IR is point-like on the scale of the galaxy. This understanding provoked a lot of work with one dimensional slit scans by the Texas group over the next few years.

A novel guiding strategy was used to precisely scan the astronomical sources across the detector array. Motion of the photometer relative to the telescope is not permitted because of changing thermal offsets. The telescope itself had to be precisely moved across the sources. The low frequency end of the telescope stabilization loop is achieved, on the KAO, by video tracking on a star in the field. We move the telescope by precisely moving the camera, which is fiber coupled to the focal plane. As the camera feed moves across the focal plane in one direction, the tracking system moves the telescope in reflection. In this way, the telescope can be scanned precisely and reproducibly in a way that is independent of the (rather poor) isoplaneticity of the video tracker camera.

The success of high spatial resolution observations with diffraction-limited slits led to new generations of instruments with diffraction-limited detector arrays. The current Harvey et al. instrument employs a 2×10^3 He cooled bolometer array. Each detector in the array is sized $\lambda/D \times \lambda/2D$, with the short axis of the detector aligned along the long axis of the array. Magnifying optics are used to make the array match the diffraction spot at either 50 or 100 μm .

The array can be scanned over bright sources, to give 2-D data (see below for Sgr A), or guided at a fixed location to give one dimensional profiles of faint sources (see below for NGC 4736).

A critical need for pushing the limits of spatial resolution on the KAO is the knowledge of, and stability of, the point source profile of the system. While at shorter wavelengths nature provides point sources in just about every field (background stars), and at longer wavelengths compact radio sources fit the bill, in the far-IR there are few reasonably bright objects that can be assumed, *a priori*, to be unresolved on a scale of a few arcseconds ($\sim \lambda/D$ in the 50, 100 μm bandpasses of the KAO photometer). As demonstrated much later by Hawkins (see below) using the KAO and IRAS, even red giants and supergiants can have far-IR structure on scales significantly larger than this. The sky is filled with sources that are intrinsically fuzzy in the far-IR, much more so than in the optical, for which point sources abound.

Solar system bodies are the only ones that are bright enough, and verifiably point like at our resolution. We have used the outer Galilean satellites (Ganymede and Callisto, sizes $\sim 1''$), Uranus ($\sim 4''$), and the brighter asteroids (Ceres and Vesta, sizes $< 1''$) for this purpose. These objects are bright enough that, in most cases, the point source profile is not the limiting factor in the deconvolution. Other bona fide point-like sources are considerably fainter, and restricting ourselves to these five objects has sometimes resulted in serious constraints on the flight plans that can be carried out.

Fortunately, the stability of the point source profile is very good. This was verified early in our work, by looking at these sources several times in the course of a flight. In practice, the PSP stability is limited by the stability of the oscillating secondary mirror, which is moving the image by as much as $10'$ at more than 20 Hz. A new oscillating secondary mirror system, installed in 1989, was an important factor in our ability to do this work.

In the following, I present a retrospective covering some of the high points of high spatial resolution far-IR studies on the KAO. While this review concentrates on diffraction-limited studies by the Texas group, it should be clear to the reader that all of the work ever done on the KAO including, in particular, that done in beamsizes of order $1'$ by the Yerkes team is, by comparison to data from IRAS or balloon, very high spatial resolution also.

FAR INFRARED EMISSION FROM GALAXIES

Because of their relatively low flux levels, galaxies present a special challenge to high resolution studies in the far-IR. The easiest targets are those that are brightest, and that strongly selects nearby objects with high luminosity. Thus, with the modest aperture of the KAO, it is star forming regions and active galaxies that have received the most attention.

In addition to those individual objects that are discussed below, diffraction-limited scans of M82 (Joy, Lester, and Harvey 1987), the prototypical Seyfert 2 galaxy NGC 1068 (Lester et al. 1987), NGC 4945 (Brock et al. 1988), and Arp 299 (Joy et al. 1989) have been made.

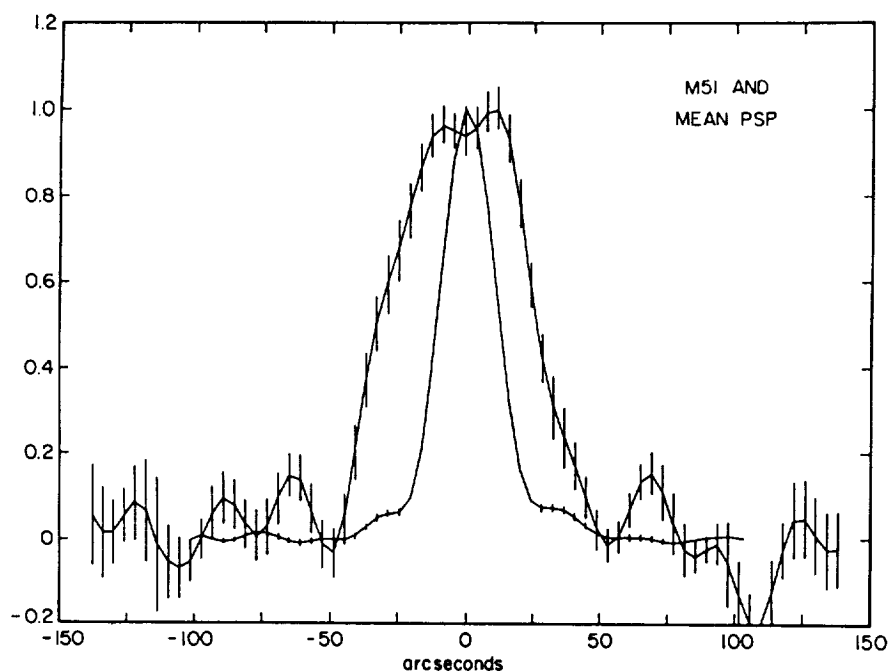


FIGURE 1 Co-added KAO slit scans at $100\ \mu\text{m}$ across the nucleus of M51 are superimposed on a point source profile from observations of Vesta. The source is clearly resolved into two components.

M51

The limits of spatial resolution in the far-IR on the KAO were first probed, in galaxies, in M51. Scans across this nearby spiral galaxy constituted a first proof of the potential of our techniques on a relatively low surface brightness source. Figure 1 (Lester, Harvey and Joy 1986) shows co-added scans across the nucleus of M51 superimposed on a point source profile from identical scans across Vesta. The source is clearly resolved into double peaks, with separation $25''$ ($120\ \text{pc}$). In the context of a slit profile, this is most simply interpreted as ring of far-IR emission with that diameter. Two deconvolution algorithms (Richardson-Lucy, and MEM) were applied to the data, and these increased the contrast in the structure that was already evident in the raw data.

This structure corresponds well with that seen in CO interferometer studies, with spiral arms wrapping around the nucleus terminating in a nearly complete ring of this size (Rand and Kulkarni 1993). This structure also very nearly envelops the older nuclear bulge of the galaxy, as delineated well by near-IR continuum images (Thronson and Greenhouse 1988). The association of this far-IR structure with star formation around the nucleus is strongly supported by the optical images of Worden (1974).

It is worth noting at this point that, while M51 has been considered a test case for IRAS imaging and deconvolution techniques, that work pertains to a

much larger scale. While the KAO observations do not have the S/N to easily detect the large scale emission (spiral arms, relationship to the companion) that is so accessible in the IRAS data, the structure that is seen in the KAO data is almost an order of magnitude smaller ($25''$ versus several arcminutes) than that available in the raw IRAS images, and a factor of several smaller than that seen in the best deconvolutions. This latter work is more comparable to the large beam KAO maps of Smith (1982).

ARP 220

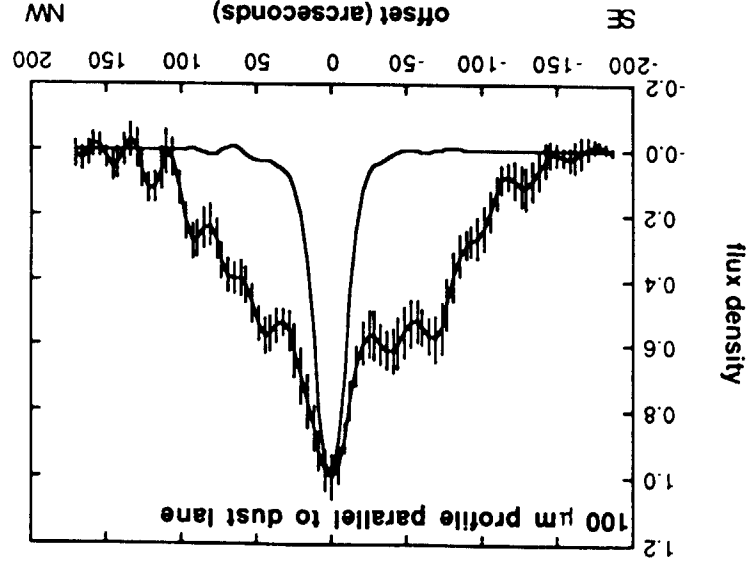
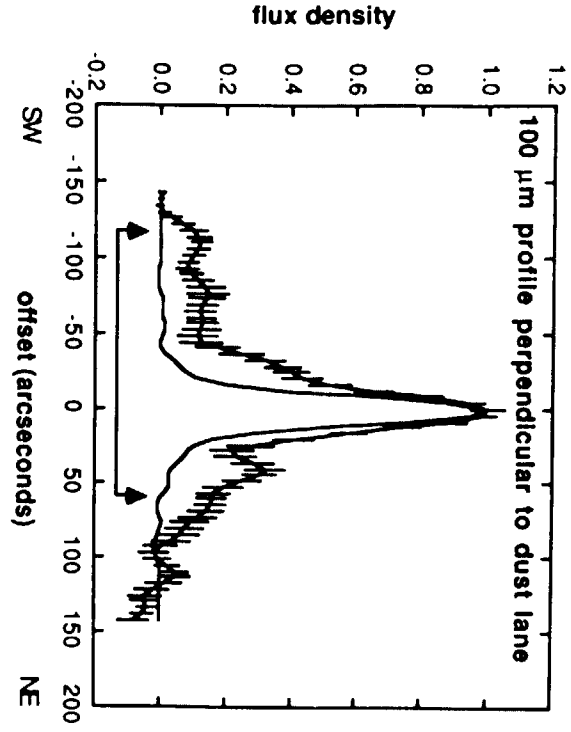
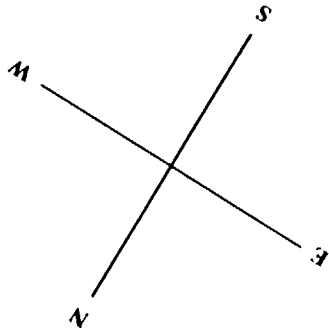
Arp 220 (IC 4553) has been characterized as an “ultraluminous” galaxy that radiates almost all of its $10^{12} L_{\odot}$ in the far-IR. There is a rich literature on this galaxy, which shows evidence for a buried AGN. The optical extent of its disk, which is highly distorted, is more than $30''$, corresponding to 10 kpc. KAO observations by Joy et al. (1986) showed conclusively, however, that the far-IR emitting region was a factor of four smaller than this, and most likely is produced in the nucleus. Using several deconvolution techniques, it was established that the $100 \mu\text{m}$ size of Arp 220 was less than $7.5''$. Using this size to compare the color temperature to the brightness temperature, a far-IR optical depth in excess of 0.05 was derived. This in turn corresponds to a visual extinction of 25–50 magnitudes, which is consistent with the fact that the high nuclear velocity dispersion that is evident in the near IR is not seen in the visible (DePoy, Becklin, and Geballe 1987).

NGC 5128 (CEN A)

Ground based studies in the mid-IR have shown that the star formation in this galaxy is strongly concentrated in the dust lane that bisects it. Presumably this giant elliptical has swallowed whole a disk galaxy, and the gas attached to this disk galaxy is now involved in a strong starburst. High resolution scans of NGC 5128 in the far-IR were made from the KAO during its 1986 deployment to New Zealand. Scans at both 50 and $100 \mu\text{m}$, perpendicular and parallel to the dust lane were obtained. The resulting profiles give a wealth of information (Joy et al. 1988). The $100 \mu\text{m}$ profiles are shown in Figure 2, where they are compared (with common scale and orientation) to an optical photograph.

The profile perpendicular to the disk (left side of figure) clearly shows that most of the far-IR emission is concentrated to the dark lane. From the mid-IR work of Telesco (1978), this is not unexpected. The extent of the far-IR emission to high z , well away from the dust lane, was not expected, and suggests that

FIGURE 2 (over) Slit scans at $100 \mu\text{m}$ parallel and perpendicular to the dust lane in NGC 5128 are scaled and oriented for comparison with an optical photograph. Three separate emission components are clearly visible—extended emission from the starburst disk along the plane, extended emission at large z distances, and emission from an unresolved point source coincident with the nonthermal nucleus. The slit length is approximately $40''$.



dust at high latitudes contributes substantially to the luminosity of this galaxy. This dust is not heated by the central source, but by star formation in situ, or perhaps by the interstellar radiation field of a quiescent bulge population. The slit scan along the dust lane shows that the star formation is fairly uniform along the disk, to the outermost optical isophote of the bulge, but shows a marked unresolved peak that is coincident with the nuclear radio source. The extended equatorial emission has a profile that is well fit by a uniform disk model, and poorly fit by a thin ring. Thus the star formation in the disk of NGC 5128 is not restricted to those bits of peripheral pieces that we can see optically, but probably covers the disk.

NGC 4736

This galaxy shows a compact, high surface brightness bulge that, while relatively blue, shows no sign of ongoing star formation. The bulge is surrounded by a ring of ionized and molecular gas with a radius of about $50''$ (1.6 kpc) that is clearly dominated by star formation. The far-IR profile across the galaxy shows striking differences compared with both the red starlight and the ionized gas. This comparison is shown in Figure 3 (Smith et al. 1991). In this face-on ringed galaxy, the morphological distinction between bulge stars (F-band profile) and star formation (H-alpha profile) is evident. Integrated-light studies of the far-IR emission from galaxies in the IRAS survey show that, while far-IR emission is dominated by star formation in many galaxies, in quiescent galaxies the far-IR emission comes from thermalization of diffuse starlight by interstellar grains. Our high resolution profiles of NGC 4736 show both mechanisms at work in different parts of the same galaxy. Note that the $100\ \mu\text{m}$ profile in this galaxy resembles neither the quiescent bulge light or the star formation in the ring closely. Unlike the H-alpha profile, the $100\ \mu\text{m}$ profile is peaked in the center. The far-IR emission from the inner parts of NGC 4736 is thus dominated by diffuse starlight. The elevation in the shoulders of the $100\ \mu\text{m}$ profile at the H-alpha ring radius shows that this emission is from star formation.

FAR INFRARED EMISSION FROM STAR FORMATION REGIONS

Unlike for galaxies, star formation regions tend to be extraordinarily bright. With a surfeit of signal-to-noise, these objects are the ones that truly push the limits of image restoration in the far-IR. In fact, it is our conclusion that, for these objects, it is our poorer understanding of the point source response function that limits our work here (solar system "point" sources are considerably fainter).

In addition to those objects described in more detail below, diffraction-limited far-IR KAO data on W3OH (Campbell et al. 1989), Cep A (Ellis et al. 1990) and Sgr B2 (Goldsmith et al. 1992) have been obtained. For the prototypical disk source S106 (Harvey et al. 1987), the KAO data suggests far-IR elongation along the disk diameter, presumably reflecting the mass morphology. Recent work by DiFrancesco et al. (1993) on Herbig Ae/Be stars shows that a majority of these stars are resolved in the far-IR on scales very much larger than that of their predicted disks.

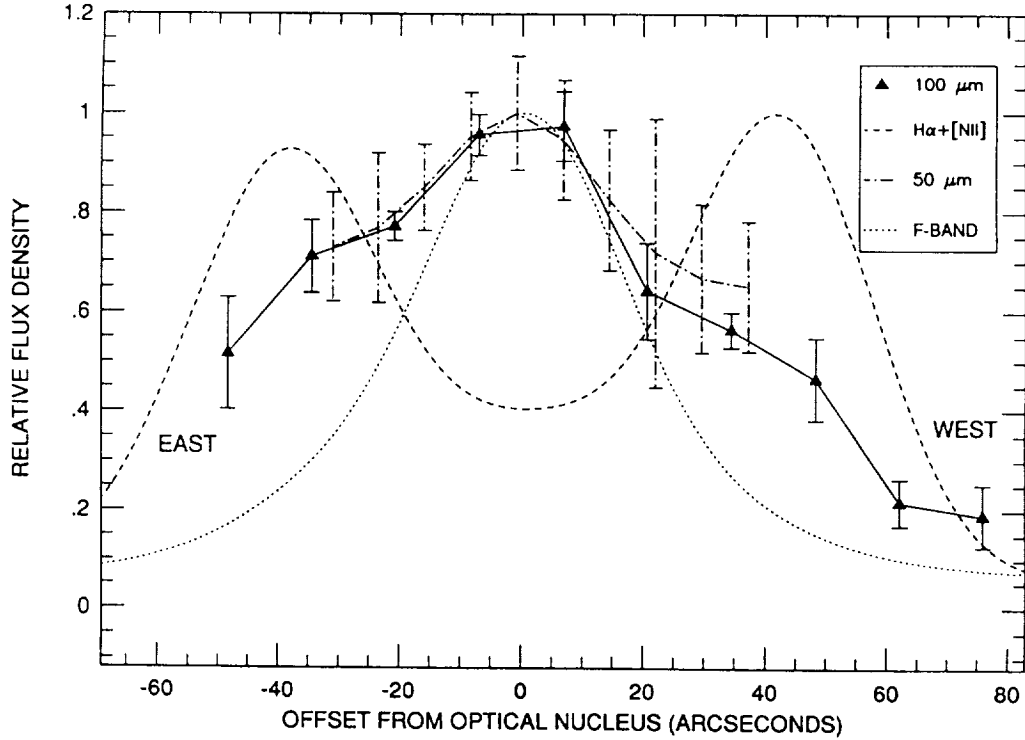


FIGURE 3 Profiles of the ringed galaxy NGC 4736. The far-IR emission follows the profile of diffuse starlight in the inner regions, yet shows enhancement at the radius of the starburst ring. Two dominant mechanisms for production of far-IR emission in galaxies are thus clearly spatially resolved for the first time in a single galaxy.

S140

Sharpless 140 was the first astronomical object studied with these techniques (Lester et al. 1986a). The temperature and density gradient across the S140 ionization front was clearly shown in these slit scans, which were oriented to sample the front with the highest resolution. In this object, the utility of Fourier “beam matching” was demonstrated, giving identically matched resolution at both 50 and 100 μm , and allowing direct ratioing of data at these two very different wavelengths.

L1551 IRS5

Slit scans along, and perpendicular to the outflow axis and putative disk in L1551 IRS5 were carried out by Butner et al. (1991). Simple deconvolution of these data show that the source is resolved on a $10''$ scale at 100 μm , fully a factor of two smaller than the diffraction spot. There is some evidence that the far-IR source is slightly elongated with the flow. Comparison of these profiles to radiative transfer codes constrain the density profile through the source.

G05.89

This remarkable compact HII region and molecular outflow source is perhaps the ultimate test for spatial resolution in the far-IR, since it is extraordinarily bright (Harvey et al. 1993). The source was barely resolved by the KAO, on scales more than a factor of two below the diffraction limits ($6''$ at $50\ \mu\text{m}$, $9''$ at $100\ \mu\text{m}$). The high far-IR surface brightness corresponds to a brightness temperature that is actually fairly similar to the color temperature, and thus the source must be optically thick in the far-IR. Comparison with radiative transfer codes indicates a $100\ \mu\text{m}$ optical depth of at least 2, and perhaps 5–10, as well as a steep density gradient. Using a canonical extinction law, visual extinctions of order several thousand are implied, making this the most optically thick source yet seen.

FAR INFRARED EMISSION FROM EVOLVED STARS

It is now well understood that many AGB stars are decidedly non-point like in the far-IR. While the work of Lester et al. (1986b) on IRC10216 indicated that much of the light from this source came from a compact region, it seems likely that a substantial fraction is emitted in this source, on a scale that is large compared to the KAO diffraction disk. The KAO work of Hawkins and Zuckerman (in preparation) shows, for example, that μ Cep is clearly resolved in the far-IR. Models of its small scale emission profile from the KAO, when compared with emission from its more extended envelope (from IRAS data) suggest large changes in the mass loss rate. It appears that the inner, more recent mass loss has been taking place at a rate about a factor of ten lower than that in the envelope.

FAR INFRARED EMISSION FROM THE GALACTIC CENTER

Recent work on Sgr A by Davidson et al. (1992) has been done from the KAO by scanning a linear array of bolometers, thus creating two-dimensional images. Application of a maximum entropy algorithm to this data produces a remarkable picture of the central few parsecs of our galaxy. The double-lobed emission there is clearly resolved, and it is centered on Sgr A*. Comparison of the KAO far-IR maps to molecular data is revealing (see Figure 4). While the molecular clouds in the vicinity of Sgr A are distributed in a ring-like structure, of diameter $\sim 3\text{pc}$, the far-IR emission is produced on the inside edge of this ring. Radiative transfer models show that the data is consistent with a flared-disk geometry inclined 60° to our line of sight, with a $0.9\ \text{pc}$ cavity at the center.

THE FUTURE OF HIGH SPATIAL RESOLUTION IN THE FAR INFRARED

Work in the last ten years has shown clearly that image restoration work from an airborne platform is highly profitable. Modest aperture diffraction limited space telescopes (ISO, SIRTf, Edison) of the future will provide enormous increases in sensitivity and, to some extent, these increases in sensitivity can be harnessed to

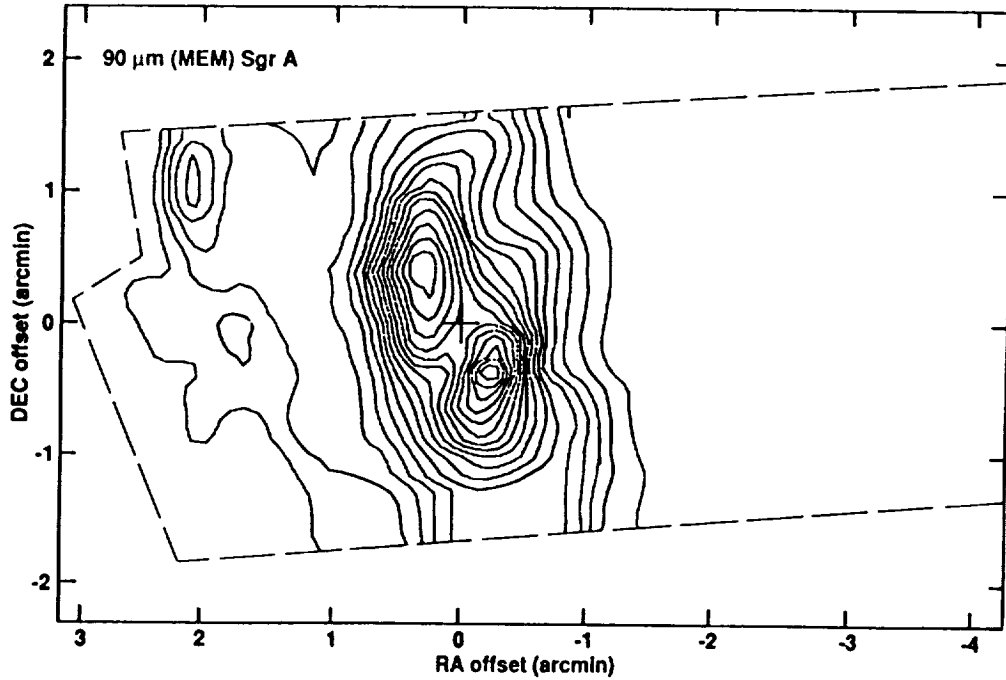


FIGURE 4 This far-IR continuum map of Sgr A was generated using a row-by-row maximum entropy image restoration routine on a map produced by scanning a linear array (1×8) of bolometers across the source. North is up and east is to the left. The beamshape in the reconstruction is roughly circular. The two far-infrared peaks in Sgr A are clearly distinguished, and are seen to have small scale elongations. This emission is nearly circumscribed by molecular gas seen in HCN and CO. The southern extension of the northern component of the pair is from a compact source, roughly coincident with IRS1, that dominates the map at shorter wavelengths.

provide, through image restoration, enhancements in spatial information. The fact remains, however, that for reasonably bright sources (and it should be noted that most of the sources that define infrared astronomy are, even in this post-IRAS era, bright sources), the biggest gain in spatial resolution comes with the largest aperture, however.

The Stratospheric Observatory for Infrared Astronomy (SOFIA) will answer this challenge. With an aperture of 2.5 m, SOFIA will provide a factor of three increase in spatial resolution over the KAO, as well as more than a factor of ten in sensitivity. For tens of thousands of the brightest far-IR sources, SOFIA will provide several times higher spatial resolution than any other space facility. Endorsed by the Bahcall panel as the highest priority new medium-price NASA mission, SOFIA is well studied, and ready to develop. With a twenty year operational lifetime, SOFIA will be used with a hundred different instruments in the course of its lifetime, each one optimized for a specific task. The accessibility of an airborne platform will, as it has for the KAO, encourage new technology that is not yet robust enough for space missions. Thus, SOFIA will always be equipped with leading-edge instrumentation. The hands-on instrumentation expertise that SOFIA will develop will be precisely that which, with a little foresight, we will need for the long-term future of high spatial resolution far-IR measurements, with large apertures in earth orbit or on the moon.

REFERENCES

- Brock, D., Joy, M., Lester, D.F., Harvey, P.M., and Ellis, H.B. Jr. 1988, *ApJ*, **329**, 208
- Butner, H.M., Evans, N.J. II, Lester, D.F., Levreault, R.M., and Strom, S.E. 1991, *ApJ*, **376**, 636
- Campbell, M.F., Lester, D.F., Harvey, P.M., and Joy, M. 1989, *ApJ*, **345**, 298
- Davidson, J.A., Werner, M.W., Wu, X., Lester, D.F., Harvey, P.M., Joy, M., Morris, M. 1992, *ApJ*, **387**, 189
- DiFrancesco et. al. 1993, in preparation
- DePoy, D., Becklin, E.E., and Geballe, T.G. 1987, *ApJ*, **316**, L63
- Ellis, H.B. Jr., Lester, D.F., Harvey, P.M., Joy, M., Telesco, C.M., Decher, R., and Werner, M.W. 1990, *ApJ*, **365**, 287
- Goldsmith, P.F., Lis, D.C., Lester, D.F., and Harvey, P.M. 1992, *ApJ*, **389**, 338
- Harvey, P.M. et al. 1993, in preparation
- Harvey, P.M., Lester, D.F., and Joy, M. 1987, *ApJ*, **316**, L75
- Hawkins and Zuckerman. 1993, in preparation
- IRAS Catalogs and Atlases: Explanatory Supplement* 1988, ed. C.A. Beichman, G. Neugebauer, H.J. Habing, P.E. Clegg, and T.J. Chester (Washington, DC: GPO)
- Joy, M., Lester, D.F., and Harvey, P.M. 1987, *ApJ*, **319**, 314
- Joy, M., Lester, D.F., Harvey, P.M., and Ellis, H.B. Jr. 1988, *ApJ*, **326**, 662

- Joy, M., Lester, D.F., Harvey, P.M., and Frueh, M. 1986, *ApJ*, **307**, 110
- Joy, M., Lester, D.F., Harvey, P.M., Telesco, C.M., Decher, R Rickard, L., and Bushouse, H. 1989, *ApJ*, **339**, 100
- Lester, D.F. July/August 1991, *Stardate Magazine*
- Lester, D.F., Harvey, P.M., and Joy, M. 1986a, *ApJ*, **302**, 280
- Lester, D.F., Harvey, P.M., and Joy, M. 1986b, *ApJ*, **304**, 623
- Lester, D.F., Joy, M., Harvey, P.M., Ellis, H.B. Jr, and Parmar, P. 1987, *ApJ*, **321**, 755
- Lester, D.F., Harvey, P.M., and Joy, M. 1986, *ApJ*, **302**, 280
- Rand, R. and Kulkarni, S. 1993, preprint
- Thronson, H., and Greenhouse, M. 1988, *ApJ*, **327**, 671
- Smith, B.J., Harvey, P.M., Colome, C., Zhang, C.Y., DiFrancesco, J., and Pogge, R.W. 1991, *ApJ*, **373**, 66
- Smith, J. 1982, *ApJ*, **261**, 463
- Telesco, C.M. 1978, *ApJ*, **226**, L125
- Worden, P. 1974, *Pub. A.S.P.*, **86**, 92